



Seeding, maturation and propagation of amyloid β -peptide aggregates in Alzheimer's disease

Xiaohang Li,^{1,†} Simona Ospitalieri,^{1,†} Tessa Robberechts,^{1,†} Linda Hofmann,² Christina Schmid,² Ajeet Rijal Upadhaya,² Marta J. Koper,^{1,3,4} Christine A. F. von Arnim,^{5,6} Sathish Kumar,⁷ Michael Willem,⁸ Kathrin Gnoth,⁹ Meine Ramakers,^{4,10} Joost Schymkowitz,^{4,10} Frederic Rousseau,^{4,10} Jochen Walter,⁷ Alicja Ronisz,¹ Karthikeyan Balakrishnan^{2,11} and Dietmar Rudolf Thal^{1,2,12}

[†]These authors contributed equally to this work.

Alzheimer's disease is neuropathologically characterized by the deposition of the amyloid β -peptide (A β) as amyloid plaques. A β plaque pathology starts in the neocortex before it propagates into further brain regions. Moreover, A β aggregates undergo maturation indicated by the occurrence of post-translational modifications. Here, we show that propagation of A β plaques is led by presumably non-modified A β followed by A β aggregate maturation. This sequence was seen neuropathologically in human brains and in amyloid precursor protein transgenic mice receiving intracerebral injections of human brain homogenates from cases varying in A β phase, A β load and A β maturation stage. The speed of propagation after seeding in mice was best related to the A β phase of the donor, the progression speed of maturation to the stage of A β aggregate maturation. Thus, different forms of A β can trigger propagation/maturation of A β aggregates, which may explain the lack of success when therapeutically targeting only specific forms of A β .

- 1 Department of Imaging and Pathology, Laboratory of Neuropathology, Leuven Brain Institute, KU-Leuven, Leuven, Belgium
- 2 Institute of Pathology, Laboratory of Neuropathology, Ulm University, Ulm, Germany
- 3 Laboratory for the Research of Neurodegenerative Diseases, Department of Neurosciences, KU-Leuven (University of Leuven), Leuven Brain Institute, Leuven, Belgium
- 4 Center for Brain and Disease Research, VIB, Leuven, Belgium
- 5 Department of Neurology, Ulm University, Ulm, Germany
- 6 Division of Geriatrics, University Medical Center Göttingen, Göttingen, Germany
- 7 Department of Neurology, University of Bonn, Bonn, Germany
- 8 Chair of Metabolic Biochemistry, Biomedical Center, Faculty of Medicine, Ludwig-Maximilians-University Munich, Munich, Germany
- 9 Department of Drug Design and Target Validation, Fraunhofer Institute for Cell Therapy and Immunology, Halle, Germany
- 10 Switch Laboratory, Department of Cellular and Molecular Medicine, KU-Leuven, Leuven, Belgium
- 11 Department of Gene Therapy, Ulm University, Ulm, Germany
- 12 Department of Pathology, UZ-Leuven, Leuven, Belgium

Correspondence to: Dietmar Rudolf Thal
Department of Imaging and Pathology
Laboratory of Neuropathology, O&N4
Box 1032, KU-Leuven, Herestraat 49
3000 Leuven, Belgium
E-mail: dietmar.thal@kuleuven.be

Keywords: amyloid β protein; Alzheimer's disease; mouse model; human brain; seeding; maturation and propagation

Abbreviations: APP = amyloid precursor protein; A β = amyloid- β ; A β _{N3pE} = N-terminally truncated and pyroglutamate modified A β ; A β _{pSer8} = phosphorylated A β ; B-A β = (biochemical) A β maturation stage; hAP score = hippocampal anterior–posterior expansion score; NFT = neurofibrillary tangles; nonAD = control cases; p-preAD = pathologically diagnosed preclinical Alzheimer's disease; p- τ = phosphorylated tau protein; symAD = symptomatic Alzheimer's disease

Introduction

Alzheimer's disease is the most frequent form of dementia in the elderly.¹ The deposition of amyloid- β peptide (A β)-containing senile plaques and the generation of neurofibrillary tangles (NFTs) composed of abnormal phosphorylated τ protein (p- τ) are the two main histopathological hallmarks of Alzheimer's disease.^{2–4} The propagation of senile plaques and NFTs from one brain region into another follows distinct hierarchical and predictable patterns.^{5,6} The sequence that describes the topographical spreading of A β -plaque pathology in the human brain is referred to as A β phases⁶ and can also be found in mouse models of A β pathology such as mutant human amyloid precursor protein (APP) overexpressing mice.⁷ Experimental evidence showed that both A β and p- τ propagate from one brain region into others by following neuronal connections.^{6,8–11}

The progression of Alzheimer's disease is also accompanied by changes in the composition of A β plaques indicated by the sequential occurrence of post-translationally modified forms of A β , which is here referred to as maturation.¹² This sequence was described as A β maturation (B-A β) stages. Newly developed A β plaques, as found in the first phase of A β deposition in the neocortex, most frequently consist only of A β that can be detected with antibodies raised against non-modified A β . Post-translationally modified forms of A β , such as N-terminal truncated and pyroglutamate modified A β (A β _{N3pE}) and phosphorylated A β (A β _{pSer8}) either occur in a later preclinical stage (A β _{N3pE}) or are mainly restricted to symptomatic Alzheimer's disease (A β _{pSer8}).^{12,13} Other authors use the term maturation in the context of the development of amyloid plaques from diffuse to cored plaques.¹⁴ Whether this maturation goes along with that of the changes in the biochemical composition (B-A β aggregate maturation) has not yet been reported in detail.

A prion-like seeding process is considered to be one of the mechanisms underlying the induction and propagation of the A β pathology in the brain.^{15,16} Moreover, transmission of A β deposition has been described in transgenic mouse models,^{17,18} non-human primates¹⁹ and patients receiving A β -positive brain extracts via human-derived growth hormone treatment, cadaveric dura grafts or previous neurosurgery.^{20–22} In these cases, A β deposition can be induced and was mainly found in blood vessels. These findings suggest that seeding of A β pathology is an important event in the pathogenesis of Alzheimer's disease and possibly involved in propagation of A β pathology throughout the brain.

Soluble and insoluble A β preparations from human Alzheimer's disease brain homogenates as well as distinct synthetic A β strains have been shown to induce seeding in a concentration-dependent manner.^{17,23–25} However, it is not yet clear whether the maturation stage of seeds has influence on seed-induced propagation and maturation of A β plaque pathology. This becomes of increasing interest in the light of antibodies against A β _{N3pE} that are now entering phase 3 trials.²⁶ Since it is theoretically possible to halt the maturation process of A β aggregate formation by tackling A β _{N3pE}, it appears

to be essential to clarify the role of A β maturation for the progression of A β plaque pathology.

Induction of A β seeding can be induced *in vitro* within A β producing, wild-type and APP-knockout hippocampal slice cultures²⁷ whereas *in vivo* seeding is restricted to animal models that overexpress APP and produce increased amounts of A β , although A β aggregates can persist in a hidden form even in APP-knockout mice.^{17,28} Thus, to study seeding of A β *in vivo*, A β producing mouse models are required.

Here, we studied the pattern of A β maturation in four different brain regions of human autopsy cases covering early as well as late affected brain regions throughout the phases of A β deposition and supplemented this descriptive analysis by functional seeding and propagation experiments in APP transgenic mice. By inducing A β seeding with patient-derived A β aggregates differing in the A β phase, A β load and B-A β aggregate maturation stage, we show that A β deposition was induced by all lysates used. In this context, the speed of propagation was associated with the amount of A β in the brain lysates and the donor A β phases whereas maturation was also influenced by the presence of A β _{N3pE} and/or A β _{pSer8} in the lysates of the donor brains.

Materials and methods

Subjects

Forty-six autopsy cases from university and municipal hospitals in Offenbach, Bonn and Ulm (Germany)^{6,12,29,30} were analysed in this study (Supplementary Table 1A and B). The autopsies were performed with informed consent of the next in kin. This study was approved by the Ulm University (54/08, 342/14) and the UZ/KU-Leuven ethical committees (S-59295, 64378).

All cases were clinically examined at the time point of hospital admission (~1–4 weeks before death) by clinicians with different specialties according to standardized protocols. These protocols included the assessment of cognitive function (orientation to place, time and person; specific cognitive or neuropsychiatric tests were not performed) and recorded the patients' ability to care for themselves and to get dressed, eating habits, bladder and bowel continence, speech patterns, writing and reading ability, short-term and long-term memory and orientation within the hospital setting. These data were used to retrospectively assess the clinical dementia rating scores for 39/46 individuals³¹ without knowledge of the pathological diagnosis. For seven cases, the available clinical data were not sufficient to obtain a clinical dementia rating score retrospectively.

Neuropathology

From all human brains, the right brain hemisphere was cut fresh and specimens were kept frozen for biochemical analysis. The left hemisphere was fixed in a 4% aqueous solution of formaldehyde or

phosphate-buffered formaldehyde for ~3–4 weeks before cutting. Brains were cut in coronal slices and screened macroscopically. For histopathological analysis and for assessing the amounts of amyloid plaques, NFTs and neuritic plaques, paraffin-embedded tissue including parts of the frontal, parietal, temporal, occipital, entorhinal cortex, the hippocampal formation at the level of the lateral geniculate body, basal ganglia, thalamus, amygdala, midbrain, pons, medulla oblongata and cerebellum were examined. Paraffin sections of 5–12 µm thickness from all blocks were stained with haematoxylin and eosin.

Data were excluded when the documentation was not clear or when tissue was not available. Cases were assigned to each group [symptomatic Alzheimer's disease (symAD); pathologically-defined preclinical Alzheimer's disease (p-preAD); non-Alzheimer's disease control (nonAD)] based on records of medical diagnosis and post-mortem neuropathological examinations (for details, see [Supplementary Table 1A](#) and [Supplementary material](#)). The sample size was determined in analogy to a previous study analysing the maturation of Aβ in the neocortex¹² and by the limitations of tissue availability (frozen samples from four brain regions of the same brain).

For neuropathological diagnosis sections were stained with immunohistochemical methods with primary antibodies against abnormal phosphorylated τ protein, Aβ_{17–24}, Aβ_{N3pE} and Aβ_{pSer8}³² ([Supplementary Table 5](#)). Primary antibodies were detected with biotinylated secondary antibodies and visualized with diaminobenzidine-HCl and the avidin-biotin complex (Vector).

The phase of Aβ plaque pathology (Aβ phase),⁶ Braak NFT stage,³³ consortium to establish a registry for Alzheimer's disease scores for neuritic plaque density,³⁴ cerebral amyloid angiopathy stage,³⁵ stage of maturation of Aβ plaques (B-Aβ plaque stage)¹² and the Aβ, Aβ_{N3pE} and Aβ_{pSer8} loads were determined (for details, please see [Supplementary material](#)).

The presence of non-modified Aβ was confirmed in cases listed in [Supplementary Table 1B](#) with an antibody (7H3D6) detecting non-truncated Aβ without phosphorylation at Ser8. This antibody does not cross-react with Aβ_{N3pE} and Aβ_{pSer8}.³²

In the temporal neocortex of Brodmann area 36, the presubicular and the cornu ammonis 1 (CA1)/subiculum region of the hippocampal formation we determined the plaque types stained with antibodies against Aβ, Aβ_{N3pE} and Aβ_{pSer8}.

Biochemistry

Biochemical analysis was carried out from 38 cases that were already included in previous studies.^{12,30} In short, protein extraction for biochemical analysis of Aβ maturation from fresh-frozen frontal neocortex (Brodmann area 6), cingulate gyrus (Brodmann area 24), putamen and the cerebellum from cases listed in [Supplementary Table 1A](#) was performed as described in detail in [Supplementary material](#). Enzyme-linked immunosorbent assay (ELISA) measurements for Aβ₄₀, Aβ₄₂, Aβ_{N3pE} and Aβ_{pSer8} were carried out without fractionation. Western blot analysis was done after separating soluble, dispersible, sodium dodecyl sulphate-soluble and formic acid soluble fractions. To detect even very low amounts of Aβ_{N3pE} and Aβ_{pSer8} the blots were detected with longer exposure times ([Supplementary material](#)).

Biochemical stages of Aβ aggregation were determined as previously published and described in detail in the [Supplementary material](#).^{3,12}

Animals

Heterozygous 2-month-old female C57BL/6J-Tg(Thy1-APPK670N;M671L)23 mice (APP23 mice) were used because they are a well-

established model for analysing Aβ seeding.^{17,25} Mice were originally generated by the Novartis Institutes for Biomedical Research (Basel, Switzerland).³⁶ For this study, we chose heterozygous female mice because they have a well predictable course of Aβ plaque pathology and start to develop the very first neocortical plaques when 5–6 months old.^{7,37,38} Thus, seeding can be easily identified by the deposition of Aβ plaque material outside the neocortex. Mice were bred by continuous backcrossing of heterozygous males with wild-type females on a C57BL/6 background in a specific pathogen free facility. All mice were housed in individual, type II filter cages with floors covered in wood shavings, with food and water *ad libitum* (for details see [Supplementary material](#)). The experimental procedures were approved by the ethical committee for animal experimentation with project number P125/2016 and carried out according to the Belgian law.

Brain extract preparation for inoculations

Fifty milligrams of fresh-frozen human brain tissue from the occipital cortex (Brodmann area 17) from the cases: symAD 2, p-preAD 2, p-preAD 14, p-preAD 21, nonAD 2 and nonAD 10 were used ([Supplementary Table 1B](#)). Tissue was homogenized in phosphate-buffered saline (PBS) using a micro-pestle (0.1 mg tissue/µl PBS) before being sonicated three times for 5 s. Next, the samples were centrifuged at 3000g for 5 min at 4°C. The supernatant was collected and stored as the total supernatant. Part of the total supernatant (i.e. initial volume for soluble and dispersible fractions) was ultracentrifuged at 121 656g for 30 min at 4°C. The resulting supernatant was further concentrated 10 times using a 3 kDa Amicon filter (Millipore) before being stored as soluble fraction. The pellet was resuspended in PBS (1/10 of the initial volume), shortly sonicated and stored as dispersible fraction. The neuropathological characterization as well as the quantitative and semi-quantitative biochemical analysis of the occipital cortex samples of these cases was carried out as described for other brain samples under the 'Neuropathology' and 'Biochemistry' sections.

The seeding activity of the brain tissue was confirmed in an *in vitro* seeding assay using mCherry-Aβ_{1–42} expressing human embryonic kidney cell line 293T (HEK293T) cells ([Supplementary material](#)).

Stereotactic injection

Sixty-nine female APP23 transgenic mice were used and randomly distributed over 11 groups ($n = 6–7$ for each group) receiving brain extracts from different cases or PBS as indicated in [Table 2](#). For stereotactic injection, 2-month-old mice were anaesthetized by intraperitoneal injection of Ketamine and Medetomidine. After placing the mice in a stereotactic frame (72-6049, Harvard Apparatus), 1 µl of brain extract was injected in the left hippocampal formation (Bregma: –2.5 mm AP, +2 mm LR, –1.8 mm DV) using a 10-µl syringe with a Hamilton needle. One mouse was injected into the right hippocampal formation (Bregma: –2.5 mm AP, –2 mm LR, –1.8 mm DV). The injection was performed at a speed of 1 µl/min. We used a separate needle and syringe for each treatment group (for more details see [Supplementary material](#)). One microlitre of the total fraction of the brain lysates represented 100 µg brain tissue. One microlitre of the soluble and dispersible fraction represented the Aβ content of 1 mg brain tissue due to the 10× concentration.

Mouse neuropathology

At 6 months of age, the mice were sacrificed by decapitation under anaesthesia with Ketamine and Medetomidine. The brains were removed

Table 1 Prevalence of plaques exhibiting A β (detected with antibodies against non-modified A β), A β _{N3pE} and A β _{pSer8} in the human brain

Brain region	Antibody	A β phase 0 (n = 9)	A β phase 1 (n = 6)	A β phase 2 (n = 8)	A β phase 3 (n = 7)	A β phase 4 (n = 3)	A β phase 5 (n = 11)
Temporal neocortex	A β	0.00	83.33	100.00	100.00	100.00	100.00
	A β _{N3pE}	0.00	66.67	87.50	87.50	100.00	100.00
	A β _{pSer8}	0.00	0.00	25.00	57.10	100.00	90.90
Cingulate gyrus	A β	0.00	0.00	62.50	100.00	100.00	100.00
	A β _{N3pE}	0.00	0.00	50.00	100.00	100.00	100.00
	A β _{pSer8}	0.00	0.00	12.50	57.10	100.00	54.50
Putamen	A β	0.00	0.00	0.00	100.00	100.00	100.00
	A β _{N3pE}	0.00	0.00	0.00	87.50	66.67	100.00
	A β _{pSer8}	0.00	0.00	0.00	0.00	33.33	36.40
Cerebellar cortex	A β	0.00	0.00	0.00	0.00	0.00	90.90
	A β _{N3pE}	0.00	0.00	0.00	0.00	0.00	90.90
	A β _{pSer8}	0.00	0.00	0.00	0.00	0.00	9.10

Percentages of cases in each A β phase exhibiting the respectively stained plaques in the human brain in the temporal neocortex (Brodmann area 36), cingulate gyrus (Brodmann area 24), putamen and cerebellar cortex are provided (n = 44 cases). A single A β phase 1 case exhibited plaques only in the occipital neocortex but not in the temporal cortex. Few A β phase 2 cases showed plaques in the entorhinal cortex/hippocampus while none were seen in the cingulate gyrus. One A β phase 5 case with A β plaques in the pons had no cerebellar plaques. Values in bold highlight positive percentage >76%.

and further processed. Brain tissue of six mice was snap-frozen and stored at -80°C . From 63 animals, the brains were kept fixed in 4% paraformaldehyde for ~4 days and embedded in paraffin. Serial sections of the mouse brain samples were immunostained using the BOND-MAX automated staining system (Leica) with polyclonal antibodies raised against A β _{1–40}³⁹ and A β _{N3pE} (Supplementary Table 4). The BOND-MAX automated staining system performs a peroxidase blocking step, incubation with primary antibody, secondary antibody, 3,3'-diaminobenzidine and a haematoxylin counterstaining via an automated protocol. Staining for A β _{pSer8} was performed with a mouse monoclonal antibody (1E4E11) (Supplementary Table 5)³² according to a staining protocol for mouse tissue with murine antibodies.⁴⁰ Briefly, the mouse primary antibodies and biotinylated anti-mouse IgG fragment antigen-binding (Fab)-fragments (Jackson ImmunoResearch Laboratories) were incubated together for 20 min (2 μg Fab-fragment for 1 μg primary antibody) at room temperature. Thereafter, normal mouse serum was added to capture unbound Fab-fragments. After epitope retrieval and subsequent peroxidase and protein blocking, the Fab-fragment linked antibodies were incubated overnight with the sections, followed by detection with horseradish peroxidase-coupled streptavidin (1/1000, 016-030-084, Jackson ImmunoResearch) and 3,3'-diaminobenzidine. Stained sections were counterstained with haematoxylin, dehydrated and mounted in Leica CV mounting medium.

Morphometric quantitative analysis of seeded amyloid- β

For A β -plaque load measurements, digital images of the hippocampal region from the injected and non-injected, plaque-free hemisphere of each mouse were taken with a Leica DM2000 LED microscope connected to a Leica DFC 700T camera at $\times 5$ magnification using the LAS V4.8 software. The images covered a total area of 4.65 mm² (reference area), the A β -positive area was measured using ImageJ software (National Institutes of Health, Bethesda, USA), and the A β -load was calculated as the percentage of the A β -positive area in the given reference area. The A β -plaque area was measured by setting a threshold based on the brightness parameter for every individual case, in a manner that the plaque area was covered. To correct for background signals of the transgenic expression of APP, we subtracted the area that was detected in the non-injected hemisphere, when applying the same threshold values as for the

injected hemisphere. For plaque load measurements, A β _{N3pE} and A β _{pSer8} positive plaques in the injected hemisphere were manually delineated with a cursor.⁴¹

To determine the spatial expansion of seeded A β plaques, the anterior–posterior extent of A β pathology was analysed for five to seven mice per group. The animals were selected for this analysis based on two inclusion criteria: (i) induction of seeding; and (ii) availability of paraffin-embedded tissue (frozen brains were not used). Spreading was analysed by scoring 12 coronal sections, covering the entire hippocampal region (-0.655 mm from Bregma until -3.78 mm from Bregma, see Supplementary Table 4 for details about the investigated levels). Scoring was performed based on absence or presence of A β pathology, separately in each section as visualized by the polyclonal anti-A β _{1–42} antibody.³⁹ The hippocampal anterior–posterior expansion score (hAP score) was calculated as a percentage of the sum of the positive sections from these 12 sections. A hAP score was also determined for anti-A β _{N3pE} and anti-A β _{pSer8}-stained sections.

Statistical analysis

Assessment and quantification of all neuropathological variables from brain samples of human cases and mice were performed by two blinded observers independently. Statistical analysis was calculated with R (v.3.6.3) and SPSS 27 (IBM, Armonk, NY, USA). The Kruskal–Wallis test with Dunn's *post hoc* method was carried out when comparing multiple groups. Friedman's test with Dunn's *post hoc* method and Bonferroni correction for multiple tests was carried out when comparing among A β , A β _{N3pE} and A β _{pSer8} pathologies, within human cases and mice pair-wise, the distribution of multiple groups. To compare A β quantification by A β loads and ELISA measurements a Spearman correlation analysis was carried out. The association of these quantitative measures with positive/negative results determined by western blotting was tested with the Mann–Whitney U-test. Spearman correlation (two-tailed) was used for comparison between seed characteristics and seeding effects in mice. Linear regression controlled for age and sex was used to determine the association of the increasing A β phase with the respective A β , A β _{N3pE} and A β _{pSer8} loads in the human brain samples. In the mouse samples we used for this purpose, an ANOVA test since all mice were female and the same age.

Table 2 Characteristics of the cases used for preparing the brain lysates used as seeds with the respective seeding performance in relation to the presence/absence, loads and expansion of induced A β , A β _{N3PE} and A β _{pSer8} deposition in mice

Cases and fraction	Induced pathology in the treated mice					Characteristics of lysates						
	Antibody	Seeded A β species ^a	Total n per group	Average A β load ^b	Average hAP score ^c	A β content, ng/ μ l	A β phase	Braak NFT stage	Temp A β load	B-A β stage	B-A β plaque stage	B-A β lysate injected
Comparison among different fractions of lysates from an Alzheimer's disease and a p-preAD case												
p-preAD2 soluble fraction	A β	50.00	6	0.037 (0.063)	13.9 (20.2)	0.011	1	1	0	0	2	0
	A β _{N3PE}	0.00		0 (0)	0 (0)							
	A β _{pSer8}	0.00		0 (0)	0 (0)							
p-preAD2 dispersible fraction	A β	50.00	6	0.021 (0.024)	27.1 (19.7)	0.009	1	1	0	0	2	0
	A β _{N3PE}	33.33		0.001 (0.001)	8.3 (11.8)							
	A β _{pSer8}	0.00		0 (0)	0 (0)							
p-preAD2 total supernatant fraction	A β	50.00	6	0.023 (0.035)	15 (22.4)	0.007	1	1	0	0	2	0
	A β _{N3PE}	0.00		0 (0)	0 (0)							
	A β _{pSer8}	0.00		0 (0)	0 (0)							
symAD2 soluble fraction	A β	83.33	6	0.266 (0.238)	66.7 (40.4)	0.017	4	4	10.88	3	3	2
	A β _{N3PE}	33.33		0.032 (0.064)	15 (33.5)							
	A β _{pSer8}	66.67		0.043 (0.061)	46.7 (44.3)							
symAD2 dispersible fraction	A β	100.00	6	0.882 (0.696)	69.4 (39.1)	0.136	4	4	10.88	3	3	2
	A β _{N3PE}	83.33		0.031 (0.028)	37.5 (34.4)							
	A β _{pSer8}	83.33		0.003 (0.002)	18.8 (14.2)							
symAD2 total supernatant fraction	A β	83.33	6	0.486 (0.611)	54.4 (45)	0.039	4	4	10.88	3	3	2
	A β _{N3PE}	33.33		0.005 (0.009)	18.1 (28.1)							
	A β _{pSer8}	50.00		0.019 (0.023)	29.2 (39.4)							
Comparison of the dispersible fraction among lysates from different cases												
PBS	A β	14.29	7	0.001 (0.003)	1.6 (4.2)		NA	NA	NA	NA	NA	NA
	A β _{N3PE}	0.00		0 (0)	0 (0)							
	A β _{pSer8}	0.00		0 (0)	0 (0)							
nonAD10	A β	0.00	7	0 (0)	0 (0)	0.001	0	0	0	0	0	0
	A β _{N3PE}	0.00		0 (0)	0 (0)							
	A β _{pSer8}	0.00		0 (0)	0 (0)							
nonAD2	A β	33.33	6	0.016 (0.024)	9.2 (14.3)	<0.001	0	1	0	0	0	0
	A β _{N3PE}	16.67		0.001 (0.002)	3.3 (8.2)							
	A β _{pSer8}	0.00		0 (0)	0 (0)							
p-preAD2	A β	50.00	6	0.021 (0.024)	27.1 (19.7)	0.009	1	1	0	0	2	0
	A β _{N3PE}	33.33		0.001 (0.001)	8.3 (11.8)							
	A β _{pSer8}	0.00		0 (0)	0 (0)							
p-preAD14	A β	100.00	7	0.23 (0.195)	36.4 (27.9)	0.031	2	2	1.54	2	3	2
	A β _{N3PE}	85.71		0.029 (0.029)	24.2 (22.2)							
	A β _{pSer8}	71.43		0.025 (0.026)	10.7 (8.6)							
p-preAD21	A β	100.00	6 ^d	2.767 (1.541)	91.7 (18.6)	0.018	5	2	5.53	2	2	2
	A β _{N3PE}	83.33		0.017 (0.012)	61.7 (32.6)							
	A β _{pSer8}	33.33		0.001 (0.002)	15 (20.7)							
symAD2	A β	100.00	6	0.882 (0.696)	69.4 (39.1)	0.136	4	4	10.88	3	3	2
	A β _{N3PE}	83.33		0.031 (0.028)	37.5 (34.4)							
	A β _{pSer8}	83.33		0.003 (0.002)	18.8 (14.2)							

n = number of animals treated for each condition. Values in bold highlight a positive percentage >76%. Note that Case p-preAD21 is exceptional since this case already showed the topographical distribution of A β phase 5 whereas A β _{pSer8} could not be detected within the plaques by immunohistochemistry. We used this case here because it allowed us to extract substantial amounts of A β in B-A β plaque stage 2. NA = not applicable.

^aValues presented as % (positive *n*/total *n*).

^bValues presented as % (\pm SD).

^cValues presented as mean (\pm SD).

^dOne mouse from this group received the injection of dispersible fraction from Case p-preAD21 in the right hippocampus.

Ethics

Ethical approval was obtained from the Ulm University Ethics Committee (Ulm/Germany; Decision No. 54/08, 342/14) and by the UZ-Leuven ethical committee (Leuven/Belgium; Decision No. S-59295, S-64378). In accordance with the Declaration of Helsinki, informed consent for autopsy and scientific use of autopsy tissue with clinical information was granted. Animal experiments were approved by the KU-Leuven ethical committee for animal experiments

(Leuven/Belgium; Decision No. P125/2016). All methods were performed in accordance with the relevant guidelines and regulations.

Data availability

All cases are listed in [Supplementary Tables 1 and 2](#) with the main parameters obtained throughout this study, with the main clinical diagnosis, age and sex. Due to legislation and privacy protection any medical reports and files of the cases included in this study cannot

be made available. Mean and standard deviations from mouse experiments are provided in Table 2. Data describing statistical results are presented in the respective figure legends, in the 'Results' section and in Supplementary Table 3. More detailed data will be provided by the corresponding author upon reasonable request.

Results

Propagation and maturation of A β plaque pathology in the human brain

To study maturation of A β plaques throughout the different phases of A β plaque propagation, 45 autopsy brains covering all A β phases were investigated (Supplementary Table 1A). We determined the composition of A β plaques in four brain regions that become subsequently affected by A β pathology: the neocortex in A β phase 1, cingulate gyrus in phase 2, basal ganglia in phase 3 and the cerebellum in phase 5 (Supplementary Table 1).⁶ In all four regions, an antibody raised against A β_{17-24} detected all A β plaques (Table 1). A subset of these plaques exhibited A β_{N3pE} -positive material in some non-demented and all demented cases. A β_{pSer8} was mainly restricted to demented cases, i.e. symAD, and only observed in cases that already exhibited A β_{N3pE} in the respective regions (Table 1). A β deposits lacking anti-A β_{N3pE} and anti-A β_{pSer8} -positivity were considered to mainly contain non-modified A β . This was supported by reactivity of A β plaques with an antibody not cross-reacting with N-terminal truncated and phosphorylated A β species³² in the cases listed in Supplementary Table 1B. The cerebellum exhibited A β_{pSer8} in only one single case. None of our cases exhibited modified forms of A β in the absence of A β detectable with antibodies raised against A β_{17-24} . The A β loads describing the area in a given region covered by A β plaques in all investigated brain regions were higher for presumably non-modified A β , than for A β_{N3pE} loads, which were higher than the respective A β_{pSer8} loads (Fig. 1). Given the A β phase-related prevalence of A β plaques in a given brain region, the temporal neocortex showed A β plaques most frequently, followed by the cingulate gyrus, then the basal ganglia and finally the cerebellum (Fig. 1, Table 1). The histopathological sequence of A β aggregate maturation from presumably non-modified A β to A β_{N3pE} and finally to A β_{pSer8} in all investigated brain regions was confirmed by western blotting and quantitative ELISA analysis of brain homogenates of the respective brain regions (Supplementary Fig. 1). The methods correlated well for detection and quantification of A β , whereas A β_{N3pE} and A β_{pSer8} were less abundant in ELISA measurements especially in the basal ganglia and the cerebellum.

The accumulation of modified A β species varied among different plaque types. Fleecy amyloid, a very early type of diffuse plaques occurring in the entorhinal cortex and the subiculum/CA1 region exhibited no A β_{N3pE} and no A β_{pSer8} (Supplementary Fig. 2A–C). Presubicular lake-like and subpial band-like amyloid were A β - and A β_{N3pE} -positive whereas A β_{pSer8} was seen there only in single cases. The highest percentage of diffuse plaques was stained with anti-A β antibodies, followed by anti-A β_{N3pE} . A β_{pSer8} was only visible in a minority of diffuse plaques (Supplementary Fig. 2). Cored plaques often exhibited all three A β forms and represented the main plaque type exhibiting A β_{pSer8} (Supplementary Fig. 2 and Supplementary Table 2).

Induction of A β seeding and maturation in APP23 mice by human brain-derived seeds from soluble and dispersible fractions of A β -containing brains

To analyse the impact of the seed (derived from different phases and maturation stages) on inducing A β deposition and maturation

in vivo, we determined first which fraction of the brain lysates (soluble or insoluble) was best suited for comparing seeds derived from different brains. To do so, we compared the seeding effects in mice injected with soluble, dispersible (insoluble) and total supernatant (soluble + dispersible) fractions (Fig. 2). To avoid contamination by p- τ pathology, we chose the Brodmann area 17 from cases with a Braak NFT stage lower than V, lacking local p- τ pathology in this region. For this purpose, we used brain lysate fractions from one A β phase 4 symAD case (Case symAD2; Supplementary Fig. 3L–N) and one A β phase 1 p-preAD case (Case p-preAD2) with single plaques in the occipital cortex (Supplementary Fig. 3C–E). The soluble, dispersible and total supernatant fractions were prepared as indicated in Fig. 2A. The proteins of the soluble and dispersible fraction were concentrated in a standardized manner to gain sufficient yield and to avoid an over-proportional enrichment of A β (see Supplementary material for details). The lysates from Case symAD2 contained ~0.017 to 0.136 ng/ μ l A β (Table 2) and detectable amounts of A β_{N3pE} whereas A β_{pSer8} could not be seen in the fractions. The fractions from Case p-preAD2 did not contain detectable amounts of A β (≤ 0.011 ng/ μ l) despite the presence of single A β plaques in the occipital cortex observed immunohistochemically (Supplementary Fig. 3). These results were confirmed by ELISA (Supplementary Fig. 3), although due to the lack of sensitivity of the antibodies and the low levels, neither A β_{N3pE} nor A β_{pSer8} was detected. To determine the seeding activity of these extracts, we used a biosensor cell model expressing mCherry-A β_{1-42} stably in HEK293T cells,⁴² and we measured mCherry-intensive spots that indicated cellular seeding. We used the sarkosyl-insoluble fractions of the selected cases in this assay. Unlike the wells that were treated with early p-preAD case (p-preAD2) extract that barely showed any positive signal, those with symAD case (symAD2) extracts exhibited A β seeding activity with a half-maximum effective concentration of 0.6083 ng/ml total A β_{1-42} (Supplementary Fig. 3T–U).

Next, the soluble, dispersible, and total supernatant fractions of the human brain lysates were injected into the left hippocampus of 2-month-old APP23 mice ($n = 6$ mice per group) (Fig. 2B). At this age, there were no A β plaques present in the hippocampus.^{7,36} To analyse the seeding effect before intrinsic A β deposition takes place in APP23 mice, we euthanized these animals at 6 months of age³⁸ and studied the seeding effect immunohistochemically with antibodies raised against (i) A β_{1-40} lacking post-translational modifications and C terminus specificity [confirmed with the 7H3D6 antibody not cross-reacting with truncated or phosphorylated A β ³² (Supplementary Fig. 4)]; (ii) A β_{N3pE} ; and (iii) A β_{pSer8} .

Nine brains from 12 mice receiving the dispersible fraction of brain lysates of the previously mentioned p-preAD and symAD cases exhibited seeded A β plaques (Table 2). A seeding effect was also observed in 16/24 of brains from animals receiving the total supernatant fraction and the soluble fraction, respectively (Table 2). All fractions from Case symAD2 induced A β , A β_{N3pE} and A β_{pSer8} deposition to a certain degree. When focusing only on presumably non-modified A β , seeding was found in all mice receiving the dispersible fraction of symAD occipital cortex (Table 2). Both the soluble and the total supernatant fraction of this case induced A β seeding in 5/6 of the respectively treated mice. When the dispersible fraction of A β phase 1 Case p-preAD2 was used to induce seeding, A β and A β_{N3pE} together were observed in two out of six mice (33%), whereas A β deposits lacking A β_{N3pE} and A β_{pSer8} were seen in three out of six (50%) of the injected animals. Total supernatant and soluble fractions of Case p-preAD2 induced a seeding effect less frequently than the dispersible fraction (Table 2A).

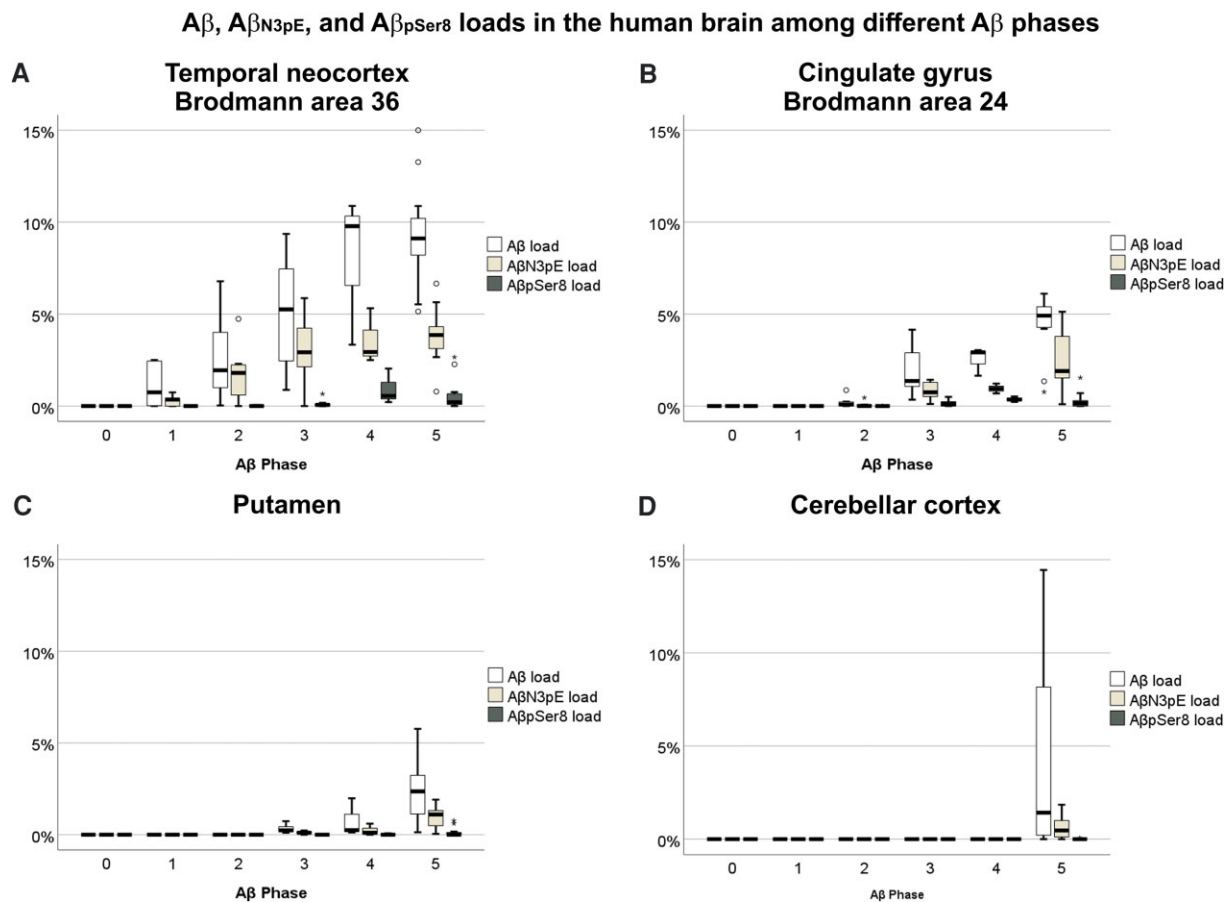


Figure 1 A β , A β _{N3pE} and A β _{pSer8} loads in the human brain among different A β phases. (A–D) Box plot diagrams comparing A β loads in the human brain among A β phases 0–5. A β , A β _{N3pE} and A β _{pSer8} loads were obtained immunohistochemically in the temporal neocortex (Brodmann area 36) (A), the cingulate gyrus (Brodmann area 24) (B), the putamen (C) and the cerebellar cortex (D) ($n = 44$). All A β , A β _{N3pE} and A β _{pSer8} loads increased with advancing A β phase as dependent variable (linear regression analysis with age and sex as additional covariates: $P < 0.05$; β : 0.289–0.731), except for the cerebellar A β _{pSer8} load (linear regression analysis with age and sex as additional covariates: $P = 0.233$). Presumably non-modified A β prevailed over A β _{N3pE} and A β _{pSer8} in the temporal cortex, cingulate gyrus and putamen [Friedman test corrected for multiple testing (two-sided): $P < 0.05$]. A β _{N3pE} was here more abundant than A β _{pSer8} [Friedman test corrected for multiple testing (two-sided): $P < 0.05$]. In the cerebellar cortex, which was only involved in A β pathology in 10 out of 11 A β phase 5 cases, presumably non-modified A β was more abundant than A β _{pSer8} [Friedman test corrected for multiple testing (two-sided): $P < 0.001$] and a trend was observed for more abundant A β _{N3pE} than A β _{pSer8} [Friedman test corrected for multiple testing (two-sided): $P = 0.059$; non-corrected $P = 0.019$]. Box elements: centre line = median; box limits = upper and lower quartiles; whiskers = 1.5 \times interquartile range; dots/stars = outliers.

The statistical comparison of the induction of seeding by the soluble, dispersible and total supernatant fractions revealed no significant differences among the fractions for the presence/absence of a seeding effect, the induced A β loads and the expansion throughout the hippocampus as measured with the hAP score (Supplementary Table 3A). Since the dispersible fraction induced seeding and maturation of A β more regularly than the soluble or total supernatant fraction, we continued with the dispersible fraction. We used it to compare the impact of seeds from brains with different levels of A β pathology, ranging from A β phase 1 to A β phase 5 and covering different biochemical stages of A β aggregate maturation on A β propagation and maturation.

Propagation- and maturation-relevant aspects of A β seeds depend on the ‘donor’s’ A β phase and maturation stage

To clarify whether the presence or absence of A β _{N3pE} and A β _{pSer8} plays a role in the capacity of brain-derived A β to induce A β seeding,

propagation and maturation we first produced dispersible fractions of brain homogenates from four human brains (Fig. 2A and B). We chose one A β phase 4 Alzheimer’s disease case (Case symAD2), one A β phase 2 p-preAD case (Case p-preAD14) with plaques exhibiting A β _{N3pE} and A β _{pSer8}, an A β phase 5 p-preAD case (Case p-preAD21) with plaques lacking A β _{pSer8} and a p-preAD case (Case p-preAD2) in A β phase 1 with single plaques containing presumably non-modified A β and A β _{N3pE} in the occipital cortex (Table 2B, Supplementary Fig. 3C and D). Biochemically, the amount of non-modified A β in the extracts was quantified by comparing the intensity of the 4 kDa bands from the extracts with standard samples containing different amounts of synthetic A β _{1–40} peptide.⁴¹ The concentrations of presumably non-modified A β in the dispersible fractions from Cases p-preAD14, p-preAD21 and symAD2 were estimated to range from 0.018 to 0.136 ng/ μ l (Supplementary Fig. 3R). These lysates contained also detectable amounts of A β _{N3pE}. A β was nearly not detectable in lysates from Case p-preAD2, nonAD10 or nonAD2 (≤ 0.009 ng/ μ l; Table 2B, Supplementary Fig. 3O–R). Lysates of control cases without A β plaques (Cases

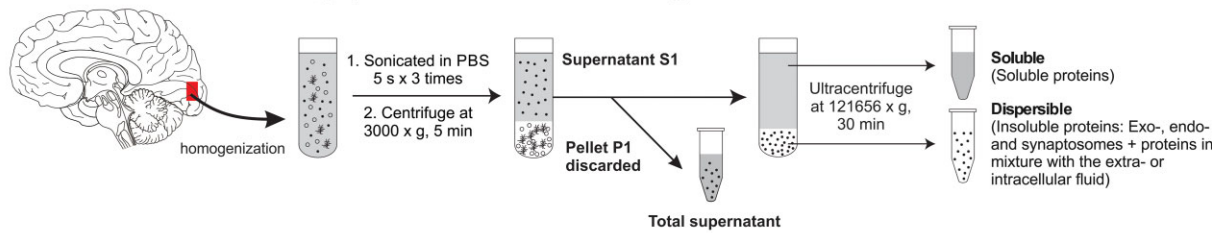
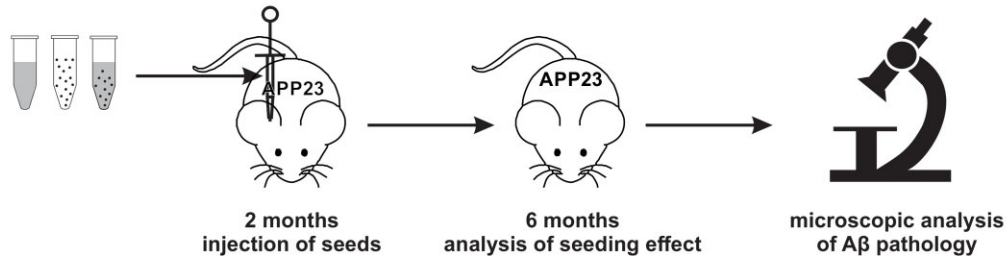
A Production of non-AD, p-preAD and AD brain homogenates for inoculation in mouse brain**B Induction of A β seeding in mouse brain by brain homogenates of non-AD, p-preAD, and symAD cases by soluble, dispersible and total supernatant fractions**

Figure 2 Propagation and maturation of A β pathology in the mouse brain after seed injection. Schematic representation of the experimental design. (A) Production of nonAD, p-preAD and Alzheimer's disease brain homogenates for inoculation in the mouse brain. For this purpose, a slightly modified centrifugation protocol according to Meyer-Luehmann et al.¹⁷ was used to generate the 'total supernatant' fractions, which was in a second step divided into soluble and insoluble but dispersible material. In short, after homogenization of occipital cortex (Brodmann area 17) samples and addition of a proteinase inhibitor cocktail, the lysates were centrifuged at 3000g. The pellet was discarded. The supernatant was considered as the total supernatant fraction. Part of the total supernatant fraction were ultracentrifuged and concentrated 10 times to separate the soluble (supernatant) and dispersible (resuspended pellet) fractions (Supplementary material). (B) Induction of A β seeding in the mouse left mouse hippocampal formation by brain homogenates of nonAD, p-preAD and symAD cases by soluble, dispersible and total supernatant fractions. To carry out this experiment, 2-month-old APP23 mice received injections of soluble, dispersible or total supernatant fractions from one sympAD and one p-preAD case. Likewise, additional mice received the dispersible fraction of two controls or two additional p-preAD cases.

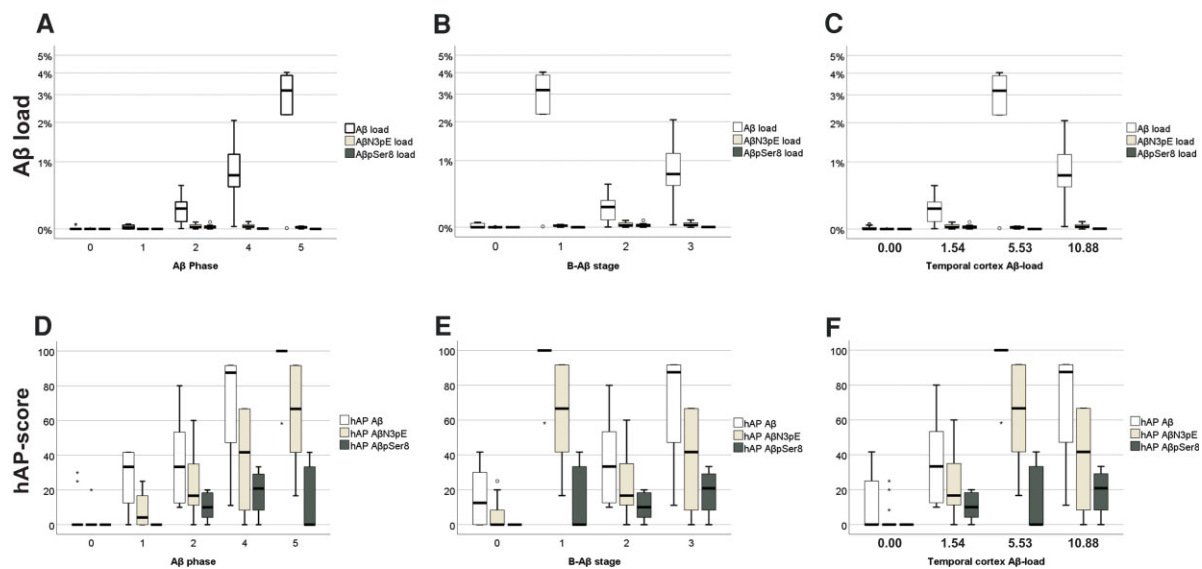


Figure 3 Relationship between 'donor' A β pathology and propagation and maturation in the 'host' brain. Box plot diagrams of the induced A β loads (A–C) and hAP scores (D–F) with the A β phases (A and D), B-A β stages (B and E) and temporal cortex A β loads (C and F), of the respective cases used for the generation of the brain lysates. ANOVA indicated an increasing tendency of the induced hAP scores for all three A β species with increasing A β phase of the injected 'donor' brains (ANOVA: $P \leq 0.023$, $n = 38$ mice) and A β load (ANOVA: $P < 0.001$, $n = 38$ mice). A β_{N3pE} and A β_{pSer8} loads did not increase continuously with A β phase although ANOVA indicated differences among the groups (ANOVA: $P \leq 0.005$, $n = 38$ mice). Increasing B-A β stages and temporal cortex A β loads of the 'donor' brains did not go along with a continuous increase of the induced A β and A β_{N3pE} loads and hAP scores and the A β_{pSer8} load, whereas the A β_{pSer8} hAP score continuously rose. Note that the A β loads and hAP scores for A β detectable with antibodies raised against non-modified forms of A β were higher than those for A β_{N3pE} and A β_{pSer8} in mice with A β pathology [Friedman test corrected for multiple testing (two-sided): $P < 0.01$, $n = 24$ mice; see also Supplementary Table 2B]. Box elements: centre line = median; box limits = upper and lower quartiles; whiskers = 1.5 \times interquartile range; dots/stars = outliers.

nonAD10 and nonAD2) were used as negative controls (Table 2, for detailed histological and biochemical characterization, and the quantification of the presumably non-modified A β , see Supplementary Fig. 30–R) as well as PBS (pH 7.6). The presence of non-modified A β species was confirmed using an antibody detecting non-truncated A β lacking phosphorylation of A β at Ser8 (Supplementary Fig. 4). The western blot-based results were confirmed by ELISA showing similar patterns of total A β_{1-40} and A β_{1-42} (Supplementary Fig. 3). In the biosensor cell model (mCherry-A β_{1-42} HEK293T cells), both p-preAD cases (p-preAD14 and p-preAD21) exhibited A β seeding activity while both nonAD cases (nonAD10 and nonAD2) showed no induction of seeding (Supplementary Fig. 3T–U).

In mice, the highest A β loads and hAP scores were induced with lysates from Case p-preAD21, followed by symAD2 and then the other p-preAD cases. In single mice, we could also observe minimal A β deposition after treatment with PBS and lysates from Case nonAD2. Since APP23 mice can develop single A β plaques ~6 months spontaneously, we would consider the minimal A β lesions in PBS and nonAD lysate-injected mice as part of the spontaneous A β deposition, maybe triggered by the minimal tissue damage caused by the injection. A similar seeding in control treated animals has also been reported by others.¹⁷ Two-tailed Spearman correlation analysis revealed that the A β phase of the donor brain was best associated with the induced A β loads and hAP propagation scores in the mice (A β load: $r = 0.842$; $P < 0.001$; hAP score: $r = 0.854$, $P < 0.001$; Fig. 3 and Supplementary Table 3B). The temporal cortex A β load, the A β_{42} content in the lysates as measured by ELISA and the B-A β stage/B-A β plaque stage of the donor also correlated with the induced A β loads and hAP scores but less well than the A β phase (Fig. 3 and Supplementary Table 3B). Thus, the speed of A β propagation as indicated by the hAP score 4 months after seeding induction showed the strongest correlation with the donor's A β phase and A β load, whereas maturation was less strongly associated.

On the contrary, the induced A β_{N3pE} and A β_{pSer8} loads and the related hAP scores correlated better with the B-A β plaque stage/B-A β stage of the donor brains (Supplementary Table 3B). The finding that brain lysates with an advanced B-A β stage induce higher hAP scores for modified forms of A β than lysates with less advanced B-A β stages indicates that the propagation of mature A β aggregates is accelerated by the presence of modified forms of A β in the seeds, i.e. the respective B-A β stage.

A β species lacking detectable amounts of A β_{N3pE} and A β_{pSer8} propagate faster than A β_{N3pE} and A β_{pSer8}

Next, we wanted to know which forms of A β expand to what extent after seeding was induced. Presumably non-modified A β deposits detected with antibodies raised against non-modified A β showed higher hAP scores than those detected with anti-A β_{N3pE} or anti-A β_{pSer8} (Supplementary Table 3C), indicating a more widespread expansion of presumably non-modified A β whereas only few A β_{N3pE} or A β_{pSer8} -positive plaques were found (Figs 3D–F and 4). In none of the mice and regardless of the fractions/lysates that were injected, A β_{N3pE} or A β_{pSer8} was found in the absence of presumably non-modified A β . Likewise, A β_{N3pE} was always present when A β_{pSer8} was detected (Figs 3 and 4 and Table 3). Since seeding and expansion of A β deposition were investigated in a 4-month interval after injecting the seeds, the more widespread distribution of presumably non-modified forms of A β represents a higher propagation speed of this A β species compared to A β_{N3pE} , which propagates still faster than A β_{pSer8} .

Discussion

The results indicate (i) that propagation of A β pathology is led by A β species lacking detectable amounts of post-translationally modified A β_{N3pE} and A β_{pSer8} in the human p-preAD and symAD brain as well as in mouse brains that were triggered to develop A β deposits by seeds from symAD or p-preAD brains; (ii) that biochemical maturation in the human brain is associated with the maturation of the plaque morphology from diffuse plaque types to mature cored ones; (iii) that maturation of A β aggregates principally takes place regardless of the origin (fraction, symAD or p-preAD brain) or biochemical composition of the brain-derived seeds but is accelerated by the presence of A β_{N3pE} and A β_{pSer8} in the seeds; and (iv) that the level of A β pathology in a given donor brain indicated by the A β phase or the A β plaque load explains the seed-induced A β extent of propagation and plaque load better than the B-A β stage of A β in the donor brain lysates. With these results, we extend the current knowledge about A β pathology propagation and maturation by highlighting the importance of presumably non-modified A β species for the induction of A β seeding and its propagation while A β maturation is accelerated by the presence of the post-translationally modified forms of A β , i.e. A β_{N3pE} and/or A β_{pSer8} . This is in line with the occurrence of A β_{N3pE} and A β_{pSer8} in more mature plaque types, especially cored plaques in Alzheimer's disease cases.

Our conclusion that presumably non-modified A β is the leading force for initiation and propagation of A β pathology in the brain is based on two independent findings: (i) the detection of A β deposits lacking A β_{N3pE} and A β_{pSer8} that occur in a given brain region before more mature forms of A β aggregates develop in each of the investigated brain regions of the human brain in symAD and p-preAD cases; and (ii) the fastest propagation of A β lacking anti-A β_{N3pE} - and anti-A β_{pSer8} -positive material in APP23 mice after induction of seeding. These findings are in line with neuropathological findings in Alzheimer's disease^{12,43} as indicated here by the lack of A β_{N3pE} and A β_{pSer8} in fleecy amyloid, which is an early plaque type preceding diffuse plaques,⁴⁴ and in A β deposits associated with normal pressure hydrocephalus.⁴⁵ They also fit with the increased propensity of A β_{N3pE} and A β_{pSer8} to form more stable and less soluble A β aggregates than non-modified A β .^{46–48} Quantitative ELISA measurements of the A β concentration in the Alzheimer's disease brain are in line and indicate that the concentration of A β_{N3pE} is more than 20 \times lower than that of A β_{42} . A β_{pSer8} is even less prominent than A β_{N3pE} and can only be detected by western blotting after long exposure of the blots. Moreover, we found that the A β composition of the lysates injected as seeds into the mice had only influence on the speed of accumulation of A β_{N3pE} and A β_{pSer8} in the seeded A β deposits but not on the deposition and propagation of other, presumably non-modified forms of A β . That brain lysates from early and late stage A β aggregates of different maturation stages induce seeding of modified A β species is further supported by our finding that even soluble A β from p-preAD cases was capable of inducing A β seeding including that of A β_{pSer8} , although soluble A β_{pSer8} was not detected in the soluble fraction.¹²

On the other hand, the accumulation of anti-A β_{N3pE} and anti-A β_{pSer8} -positive material is essential for the maturation of A β , which is linked with the development of cognitive decline in Alzheimer's disease cases compared to non-demented individuals¹² and to p- τ pathology.⁴⁹ In this context, the presence of anti-A β_{N3pE} and anti-A β_{pSer8} -positive material in seeds accelerated the accumulation of the post-translationally modified forms of A β as indicated by the respective A β_{N3pE} - and A β_{pSer8} -loads.

As expected from earlier studies using mouse brain-derived A β , the concentration of A β in the seeds determined the severity of the

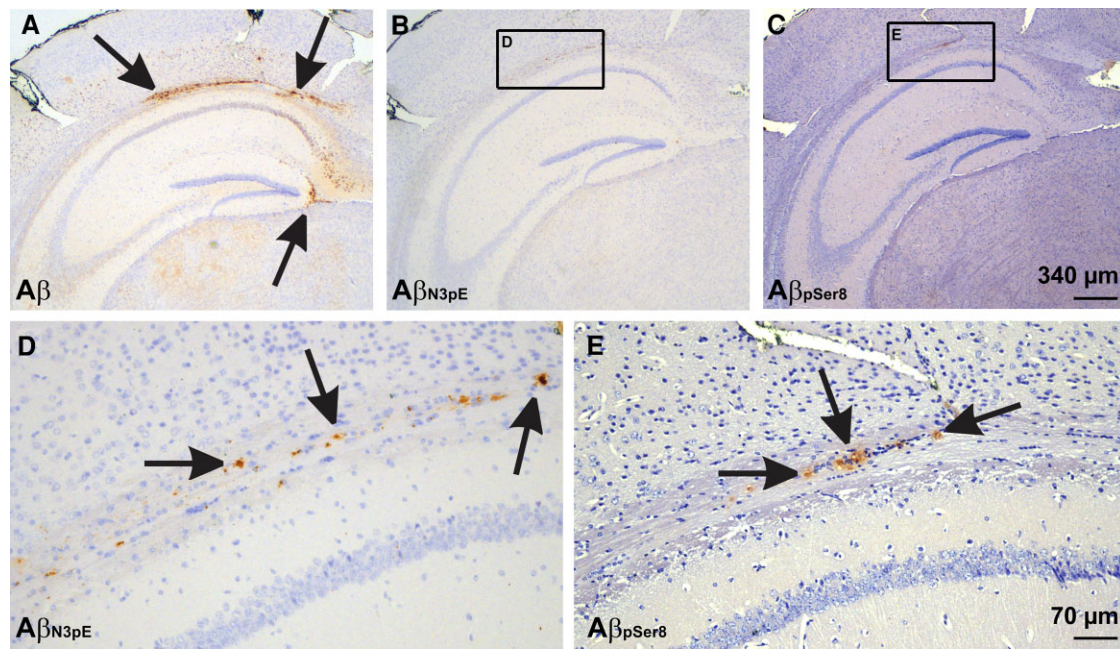


Figure 4 Seeded A β in mice receiving the dispersible fraction from p-preAD case 14. (A) Seeded plaques stained with a non-C terminus-specific polyclonal antibody raised against A β_{1-40} . The A β deposits were easily detectable even at low magnification level. (B and C) At low magnification level A β_{N3pE} - and A β_{pSer8} -positive plaques were less widespread and less visible. Calibration bar in C is valid for A–C. (D and E) At high power magnification both A β_{N3pE} and A β_{pSer8} was seen at the white matter next to the hippocampal sector CA1. Note that A β_{N3pE} -positive material was more widely distributed compared to A β_{pSer8} . Calibration bar in E is valid for D and E.

seeding effect.^{50,25} In our study, the concentration of A β in the brain measured by ELISA corresponds to the A β loads and the phases of A β deposition in the brains of the individuals used to produce the lysates for inducing seeding. Interestingly, even brain lysates from an A β phase 1 p-preAD case induced a mild seeding effect in 50% of the mice receiving the lysates whereas plaque-free lysates from younger individuals did not induce significant seeding. Since all lysates were prepared in an identical procedure, their seeding activity is related to the concentration of the relevant A β forms in the respective samples that varied among the cases. This was confirmed in our *in vitro* seeding assay and extends earlier reports about seeding with Alzheimer's disease and A β containing brain lysates from non-demented individuals⁵¹ by clearly indicating that p-preAD cases already have a seeding capacity, i.e. the capacity to kick-off the process of Alzheimer's disease-related β -amyloidosis. By doing so, we deliver another argument supporting the hypothesis that A β deposition in the human brain represents one pathological process that begins with the very first A β plaques in the neocortex of non-demented individuals and ends in symAD. Other arguments are the hierarchical pattern of A β deposition and propagation in the human brain⁶ that is reflected

by the progression of A β PET tracer retention with increasing A β phase over time^{52–54} and by the sequence of A β deposition in the brains of APP transgenic mice.⁷ Altogether, these arguments strongly support the idea that A β plaque deposition, whenever present in the human brain, represents Alzheimer's disease-related β -amyloidosis even when the concentration of A β was not significantly increased as in A β phase 1.

Moreover, we found that the speed of propagation of seeded A β correlates with A β phase, A β plaque load and A β concentration of the donor brain and the progression speed of maturation with the B-A β stage of A β aggregate maturation. This finding indicates that these two aspects of A β pathology, propagation and maturation, both influence the speed of disease progression. Thus, biomarkers for modified forms of A β may help to provide a better prognosis for non-demented individuals with positive amyloid biomarkers because they would add information about a second aspect, i.e. the status of A β maturation in the brain.

This study has limitations that need to be mentioned: (i) the number of human autopsy cases used for determining the propagation patterns of A β aggregates in the human brain is not very high ($n = 45$); (ii) the number of cases used for the preparation of brain

Table 3 Percentages of mice with seeded A β lesions exhibiting all three types of A β

	A β	A β + A β_{N3pE}	A β + A β_{N3pE} + A β_{pSer8}	A β_{N3pE} + A β_{pSer8}	A β_{pSer8}	A β_{N3pE}
Soluble fraction	50% ($n = 4$)	25% ($n = 2$)	25% ($n = 2$)	0% ($n = 0$)	0% ($n = 0$)	0% ($n = 0$)
Dispersible fraction	20.8% ($n = 5$)	29.2% ($n = 7$)	50% ($n = 12$)	0% ($n = 0$)	0% ($n = 0$)	0% ($n = 0$)
Total fraction	62.5% ($n = 5$)	12.5% ($n = 1$)	25% ($n = 2$)	0% ($n = 0$)	0% ($n = 0$)	0% ($n = 0$)

Values with a positive percentage between 50 and 74% are highlighted in bold. The table indicates the percentages of mice with seeded A β lesions exhibiting all three types of A β (A β , A β_{N3pE} and A β_{pSer8}), A β lesions lacking A β_{N3pE} and A β_{pSer8} , and A β lesions showing only A β and A β_{N3pE} but no A β_{pSer8} . We did not observe A β_{N3pE} and A β_{pSer8} in the absence of non-modified A β and A β_{pSer8} without coexisting A β and A β_{N3pE} . It is interesting to note that injection of the dispersible fraction induced more frequently the induction of all types of A β species whereas injection of the soluble and total fraction led mainly to the induction A β lacking A β_{N3pE} and A β_{pSer8} .

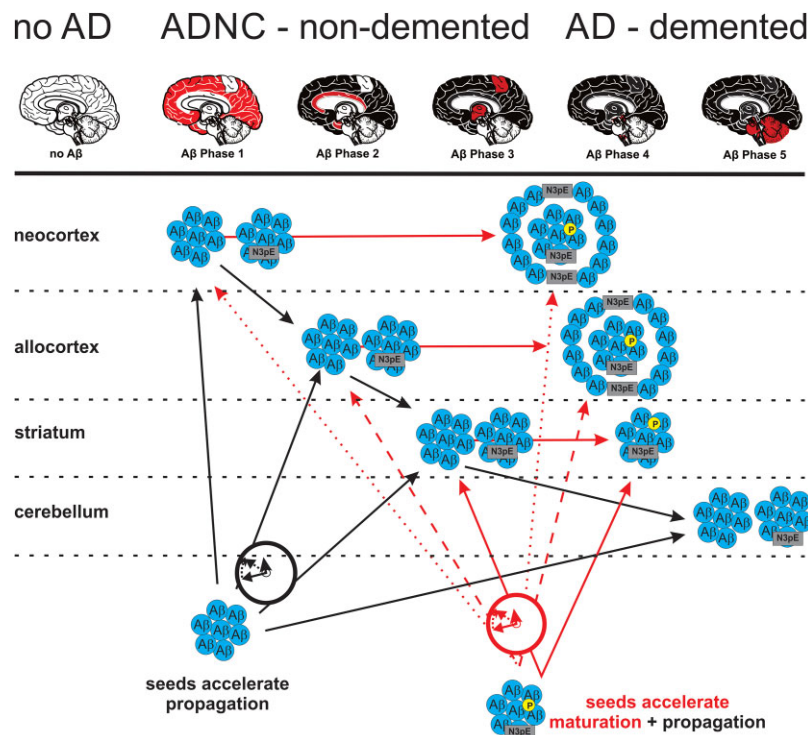


Figure 5 Schematic representation of A β protein deposition, propagation, maturation and its acceleration by seeds. Although A β propagation and maturation correlate with one another³⁰ acceleration of these two aspects in the pathogenesis of Alzheimer's disease is modified in a differential manner: propagation of A β deposition is accelerated by any kind of A β seeds whereas maturation increase depends on the presence of A β _{N3pE} and A β _{pSer8} in the seeds in a biochemically detectable concentration. Note that A β _{pSer8}-positive plaques are mainly cored plaques.

lysates for the induction of seeding in mice is low ($n=6$); (iii) the antibodies raised against non-modified A β , A β _{N3pE} and A β _{pSer8} may vary slightly in their affinity for the respective A β variants; and (iv) the seeding effect in the mice can only be measured by morphological methods since a biochemical distinction between injected human A β and the transgenically produced human A β in APP23 mice is not possible.¹⁷ Regarding these limitations, we wish to clarify that the number of human cases investigated here is in the range of similar studies and sufficient from a statistical point of view.^{17,55,56} Moreover, the cases have been investigated immunohistochemically and biochemically to confirm the results obtained with one method by a second one. The animal experiments confirm on top of it the finding of a pivotal role of presumably non-modified A β in A β propagation. Statistical analysis confirmed the validity of our findings. The sensitivity of the anti-A β _{17–24}, anti-A β _{N3pE} and anti-A β _{pSer8} antibodies range between 5 and 25 ng/ml but was optimized by the respective antibody concentrations used for staining (Supplementary Table 5). ELISAs can provide high quality quantitative data; however, the amount of A β _{N3pE} and especially A β _{pSer8} in our extracts was close to the detection threshold with a high signal to noise ratio (Supplementary Fig. 1C). Accordingly, these ELISA results could only complement the western blots and the immunohistochemical results. Moreover, other authors published similar results regarding the subsequent staining with the antibodies against differently modified forms of A β .^{43,45,49,57} In addition, we used a biosensor cell model to determine A β seeding activity of extracts from cases of different A β phases *in vitro*. By doing so, we minimized the impact of the limitations in this study as much as possible.

Given the impact of both, A β pathology propagation and maturation, for the progression of A β pathology from p-preAD to symAD,

there are several suggestions for optimizing A β targeting treatment strategies. Currently, active and passive vaccination strategies mainly target distinct forms of A β or its aggregates, such as pyroglutamate modified A β _{N3pE} (donanemab²⁶) or soluble oligomeric and insoluble fibrillar A β aggregates (aducanumab⁵⁸). Accordingly, other forms are not targeted. Given our finding that different forms of A β aggregates may be able to induce/influence seeding, propagation and/or maturation of A β , targeting only one species may be not enough to stop the complex process of A β pathology in the brain. However, an option could be focusing on blocking A β maturation rather than stopping its propagation, e.g. by targeting A β species that are restricted to mature A β aggregates. For example, donanemab, an antibody targeting A β _{N3pE}, could be such a maturation blocker.²⁶ A combination of a potential propagation stopper and a maturation blocker could offer synergy effects on counteracting A β pathology by interfering, for example, with soluble, diffusible aggregates⁵⁸ and modified A β _{N3pE}²⁶ at the same time. However, this would mean that propagation of A β pathology determined by amyloid PET or pan-A β biomarkers would probably not be optimally suited to monitor the success of such a treatment rather than using additional A β _{N3pE}- and/or A β _{pSer8}-specific biomarkers and the clinical outcome. It will also be important to keep in mind that residual A β aggregates that escaped, for example, peripherally administered antibodies can still accelerate propagation and/or maturation of A β aggregates to a certain extent as shown here by the seeding effect of an A β phase 1 p-preAD case. Thus, a potentially general problem of all passive immunization strategies is the survival of seeds that can continue or restart the process of A β propagation and maturation. Active vaccination strategies targeting multiple forms of A β started in the preclinical phase could be an alternative for future Alzheimer's disease treatment as well as combination therapies with secretase

inhibitors. Thus, re-evaluation of clinical trials using passive and active vaccination against A β considering the aspects of A β maturation and propagation separately could help to understand why vaccination strategies did not work as good as primarily expected and whether polyvaccination against multiple forms of A β could be an option for future trials. In doing so, our findings on the different A β forms involved in A β propagation provide novel insights for identifying critical aspects in targeting A β sufficiently by showing potential ‘escape routes’ for A β to allow a re-entering into the vicious cycle of A β aggregation, propagation and maturation (Fig. 5).

Acknowledgements

The authors thank Irina Kosterin for technical support and Dr A. Piechotta for supporting the production of the J8 anti-A β _{N3pE} antibody.

Funding

This study was supported by Fonds Wetenschappelijk Onderzoek Vlaanderen [FWO- G0F8516N, G065721N (D.R.T.)], Deutsche Forschungsgemeinschaft [TH624-6-1 (D.R.T.) and WA 1477/6-6 (J.W.)] and Alzheimer Forschung Initiative [#10810 (D.R.T.) and #17011 (S.K.)]. The Switch Laboratory was supported by the Flanders Institute for Biotechnology (VIB); KU-Leuven; the Fonds Wetenschappelijk Onderzoek Vlaanderen (FWO, project grant G0C3522N, FWO/Hercules equipment grant NextGenQBio—AH2016.133); the Stichting Alzheimer Onderzoek (SAO-FRA 2020/0009).

Competing interests

C.A.F.v.A. received honoraria from serving on the scientific advisory board of Biogen, Roche and Dr Willmar Schwabe GmbH & Co. KG, has received funding for travel and speaker honoraria from Biogen, Roche Diagnostics AG and Dr Willmar Schwabe GmbH & Co. KG and has received research support from Roche Diagnostics AG. D.R.T. received speaker honoraria from Novartis Pharma Basel (Switzerland) and Biogen (USA), travel reimbursement from GE-Healthcare (UK) and UCB (Belgium), and collaborated with GE-Healthcare (UK), Novartis Pharma Basel (Switzerland), Probiobdrug (Germany) and Janssen Pharmaceutical Companies (Belgium). D.R.T. received additional funding from Stichting Alzheimer Onderzoek (Belgium) in the context of another project and serves in the editorial board of *Brain* but was not involved in the handling of this manuscript at any stage.

Supplementary material

Supplementary material is available at *Brain* online.

References

- Alzheimer's Association. 2016 Alzheimer's disease facts and figures. *Alzheimers Dement*. 2016;12: 459–509.
- Alzheimer A. Über eine eigenartige Erkrankung der Hirnrinde. *Allg Zschr Psych*. 1907;64:146–148.
- Masters CL, Simms G, Weinman NA, Multhaup G, McDonald BL, Beyreuther K. Amyloid plaque core protein in Alzheimer disease and Down syndrome. *Proc Natl Acad Sci USA*. 1985;82:4245–4249.
- Grundke-Iqbal I, Iqbal K, Quinlan M, Tung YC, Zaidi MS, Wisniewski HM. Microtubule-associated protein tau. A component of Alzheimer paired helical filaments. *J Biol Chem* 1986;261: 6084–6089.
- Braak H, Braak E. Neuropathological staging of Alzheimer-related changes. *Acta Neuropathol*. 1991;82:239–259.
- Thal DR, Rüb U, Orantes M, Braak H. Phases of Abeta-deposition in the human brain and its relevance for the development of AD. *Neurology*. 2002;58:1791–1800.
- Thal DR, Capetillo-Zarate E, Del Tredici K, Braak H. The development of amyloid beta protein deposits in the aged brain. *Sci Aging Knowledge Environ*. 2006;2006:re1.
- Braak H, Del Tredici K. Alzheimer's pathogenesis: is there neuron-to-neuron propagation? *Acta Neuropathol*. 2011;121:589–595.
- Calafate S, Buist A, Miskiewicz K, et al. Synaptic contacts enhance cell-to-cell tau pathology propagation. *Cell Rep*. 2015;11:1176–1183.
- Iba M, McBride JD, Guo JL, Zhang B, Trojanowski JQ, Lee VM. Tau pathology spread in PS19 tau transgenic mice following locus coeruleus (LC) injections of synthetic tau fibrils is determined by the LC's afferent and efferent connections. *Acta Neuropathol*. 2015;130:349–362.
- Ye L, Hamaguchi T, Fritschi SK, et al. Progression of seed-induced abeta deposition within the limbic connectome. *Brain Pathol*. 2015;25:743–752.
- Rijal Upadhaya A, Kosterin I, Kumar S, et al. Biochemical stages of amyloid β -peptide aggregation and accumulation in the human brain and their association with symptomatic and pathologically-preclinical Alzheimer's disease. *Brain*. 2014;137:887–903.
- Gerth J, Kumar S, Rijal Upadhaya A, et al. Modified amyloid variants in pathological subgroups of beta-amyloidosis. *Ann Clin Transl Neurol*. 2018;5:815–831.
- Dickson DW. The pathogenesis of senile plaques. *J Neuropathol Exp Neurol*. 1997;56:321–339.
- Jucker M, Walker LC. Self-propagation of pathogenic protein aggregates in neurodegenerative diseases. *Nature*. 2013;501:45–51.
- Peng C, Trojanowski JQ, Lee VM. Protein transmission in neurodegenerative disease. *Nat Rev Neurol*. 2020;16:199–212.
- Meyer-Luehmann M, Coomaraswamy J, Bolmont T, et al. Exogenous induction of cerebral beta-amyloidogenesis is governed by agent and host. *Science*. 2006;313:1781–1784.
- Herard AS, Petit F, Gary C, et al. Induction of amyloid-beta deposits from serially transmitted, histologically silent, abeta seeds issued from human brains. *Acta Neuropathol Commun*. 2020;8:205.
- Gary C, Lam S, Herard AS, et al. Encephalopathy induced by Alzheimer brain inoculation in a non-human primate. *Acta Neuropathol Commun*. 2019;7:126.
- Jaunmuktane Z, Mead S, Ellis M, et al. Evidence for human transmission of amyloid-beta pathology and cerebral amyloid angiopathy. *Nature*. 2015;525:247–250.
- Cali I, Cohen ML, Haik S, et al. Iatrogenic Creutzfeldt-Jakob disease with amyloid-beta pathology: An international study. *Acta Neuropathol Commun*. 2018;6:5.
- Jaunmuktane Z, Quaegebeur A, Taipa R, et al. Evidence of amyloid-beta cerebral amyloid angiopathy transmission through neurosurgery. *Acta Neuropathol*. 2018;135:671–679.
- Langer F, Eisele YS, Fritschi SK, Staufenbiel M, Walker LC, Jucker M. Soluble abeta seeds are potent inducers of cerebral beta-amyloid deposition. *J Neurosci*. 2011;31:14488–14495.
- Stohr J, Condello C, Watts JC, et al. Distinct synthetic abeta prion strains producing different amyloid deposits in bigenic mice. *Proc Natl Acad Sci USA*. 2014;111:10329–10334.
- Ye L, Rasmussen J, Kaeser SA, et al. Abeta seeding potency peaks in the early stages of cerebral beta-amyloidosis. *EMBO Rep*. 2017; 18:1536–1544.

26. Mintun MA, Lo AC, Duggan Evans C, et al. Donanemab in early Alzheimer's disease. *N Engl J Med*. 2021;384:1691–1704.
27. Novotny R, Langer F, Mahler J, et al. Conversion of synthetic Aβ to in vivo active seeds and amyloid plaque formation in a hippocampal slice culture model. *J Neurosci*. 2016;36: 5084–5093.
28. Ye L, Fritschy SK, Schelle J, et al. Persistence of Aβ seeds in APP null mouse brain. *Nat Neurosci*. 2015;18:1559–1561.
29. Thal DR, von Arnim C, Griffin WS, et al. Pathology of clinical and preclinical Alzheimer's disease. *Eur Arch Psychiatry Clin Neurosci*. 2013;263:S137–S145.
30. Thal DR, Ronisz A, Tousseyn T, et al. Different aspects of Alzheimer's disease-related amyloid beta-peptide pathology and their relationship to amyloid positron emission tomography imaging and dementia. *Acta Neuropathol Commun*. 2019;7:178.
31. Hughes CP, Berg L, Danziger WL, Coben LA, Martin RL. A new clinical scale for the staging of dementia. *Br J Psychiatry*. 1982; 140:566–572.
32. Kumar S, Wirths O, Theil S, Gerth J, Bayer TA, Walter J. Early intraneuronal accumulation and increased aggregation of phosphorylated Aβ in a mouse model of Alzheimer's disease. *Acta Neuropathol*. 2013;125:699–709.
33. Braak H, Alafuzoff I, Arzberger T, Kretschmar H, Del Tredici K. Staging of Alzheimer disease-associated neurofibrillary pathology using paraffin sections and immunocytochemistry. *Acta Neuropathol*. 2006;112:389–404.
34. Mirra SS, Heyman A, McKeel D, et al. The Consortium to Establish a Registry for Alzheimer's Disease (CERAD). Part II. Standardization of the neuropathologic assessment of Alzheimer's disease. *Neurology*. 1991;41:479–486.
35. Thal DR, Ghebremedhin E, Orantes M, Wiestler OD. Vascular pathology in Alzheimer's disease: correlation of cerebral amyloid angiopathy and arteriosclerosis/lipohyalinosis with cognitive decline. *J Neuropathol Exp Neurol*. 2003;62:1287–1301.
36. Sturchler-Pierrat C, Abramowski D, Duke M, et al. Two amyloid precursor protein transgenic mouse models with Alzheimer disease-like pathology. *Proc Natl Acad Sci USA*. 1997;94:13287–13292.
37. Sturchler-Pierrat C, Staufienbiel M. Pathogenic mechanisms of Alzheimer's disease analyzed in the APP23 transgenic mouse model. *Ann N Y Acad Sci*. 2000;920:134–139.
38. Capetillo-Zarate E, Staufienbiel M, Abramowski D, et al. Selective vulnerability of different types of commissural neurons for amyloid beta-protein induced neurodegeneration in APP23 mice correlates with dendritic tree morphology. *Brain*. 2006; 129:2992–3005.
39. Page RM, Gutsmedl A, Fukumori A, Winkler E, Haass C, Steiner H. Beta-amyloid precursor protein mutants respond to gamma-secretase modulators. *J Biol Chem*. 2010;285:17798–17810.
40. Goodpaster T, Randolph-Habecker J. A flexible mouse-on-mouse immunohistochemical staining technique adaptable to biotin-free reagents, immunofluorescence, and multiple antibody staining. *J Histochem Cytochem*. 2014;62:197–204.
41. Rijal Upadhaya A, Capetillo-Zarate E, Kosterin I, et al. Dispersible amyloid β-protein oligomers, protofibrils, and fibrils represent diffusible but not soluble aggregates: Their role in neurodegeneration in amyloid precursor protein (APP) transgenic mice. *Neurobiol Aging*. 2012;33:2641–2660.
42. Konstantoulea K, Guerreiro P, Ramakers M, et al. Heterotypic amyloid beta interactions facilitate amyloid assembly and modify amyloid structure. *EMBO J*. 2022;41:e108591.
43. Ashby EL, Miners JS, Kumar S, Walter J, Love S, Kehoe PG. Investigation of Aβ phosphorylated at serine 8 (pAβ) in Alzheimer's disease, dementia with Lewy bodies and vascular dementia. *Neuropathol Appl Neurobiol*. 2015;41:428–444.
44. Thal DR, Sassin I, Schultz C, Haass C, Braak E, Braak H. Fleecy amyloid deposits in the internal layers of the human entorhinal cortex are comprised of N-terminal truncated fragments of Aβ. *J Neuropathol Exp Neurol*. 1999;58:210–216.
45. Libard S, Walter J, Alafuzoff I. In vivo characterization of biochemical variants of amyloid-beta in subjects with idiopathic normal pressure hydrocephalus and Alzheimer's disease neuropathological change. *J Alzheimers Dis*. 2021;80:1003–1012.
46. Schlenzig D, Manhart S, Cinar Y, et al. Pyroglutamate formation influences solubility and amyloidogenicity of amyloid peptides. *Biochemistry*. 2009;48:7072–7078.
47. Kumar S, Rezaei-Ghaleh N, Terwel D, et al. Extracellular phosphorylation of the amyloid beta-peptide promotes formation of toxic aggregates during the pathogenesis of Alzheimer's disease. *EMBO J*. 2011;30:2255–2265.
48. Rezaei-Ghaleh N, Amininasab M, Kumar S, Walter J, Zweckstetter M. Phosphorylation modifies the molecular stability of beta-amyloid deposits. *Nat Commun*. 2016;7:11359.
49. Mandler M, Walker L, Santic R, et al. Pyroglutamylated amyloid-beta is associated with hyperphosphorylated tau and severity of Alzheimer's disease. *Acta Neuropathol*. 2014;128:67–79.
50. Morales R, Bravo-Alegria J, Duran-Aniotz C, Soto C. Titration of biologically active amyloid-beta seeds in a transgenic mouse model of Alzheimer's disease. *Sci Rep*. 2015;5:9349.
51. Duran-Aniotz C, Morales R, Moreno-Gonzalez I, Hu PP, Soto C. Brains from non-Alzheimer's individuals containing amyloid deposits accelerate Aβ deposition in vivo. *Acta Neuropathol Commun*. 2013;1:76.
52. Grothe MJ, Barthel H, Sepulcre J, et al. In vivo staging of regional amyloid deposition. *Neurology*. 2017;89:2031–2038.
53. Hanseeuw BJ, Betensky RA, Mormino EC, et al. PET staging of amyloidosis using striatum. *Alzheimers Dement*. 2018;14:1281–1292.
54. Thal DR, Beach TG, Zanette M, et al. Estimation of amyloid distribution by [(18)F]flutemetamol PET predicts the neuropathological phase of amyloid beta-protein deposition. *Acta Neuropathol*. 2018;136:557–567.
55. Gomes LA, Hipp SA, Rijal Upadhaya A, et al. Aβ-induced acceleration of Alzheimer-related tau-pathology spreading and its association with prion protein. *Acta Neuropathol*. 2019;138:913–941.
56. Ruan Z, Pathak D, Venkatesan Kalavai S, et al. Alzheimer's disease brain-derived extracellular vesicles spread tau pathology in interneurons. *Brain*. 2021;144:288–309.
57. Lemere CA, Blusztajn JK, Yamaguchi H, Wisniewski T, Saido TC, Selkoe DJ. Sequence of deposition of heterogeneous amyloid beta-peptides and APO E in down syndrome: Implications for initial events in amyloid plaque formation. *Neurobiol Dis*. 1996;3:16–32.
58. Sevigny J, Chiao P, Bussiere T, et al. The antibody aducanumab reduces Aβ plaques in Alzheimer's disease. *Nature*. 2016; 537:50–56.